ADVANCED ELECTRONIC MATERIALS Open Access
www.advelectronicmat.de

Flexible Artificial Mechanoreceptor Based on Microwave Annealed Morphotropic Phase Boundary of $Hf_xZr_{1-x}O_2$ Thin Film

*Minhyun Jung, Seungyeob Kim, Junghyeon Hwang, Hye Jin Kim, Yunjeong Kim, Jinho Ahn, and Sanghun Jeon**

The development of artificial tactile receptor systems is important in the fields of prosthetic devices, interfaces for the metaverse, and sensors. A pressure sensor and memory device may be used in this system to replicate the tactile detecting capabilities of human skin. The implementation of systems that take into account mass production and miniaturization is still difficult. Here, a flexible artificial tactile receptor built using conventional semiconductor processes that combine a vertically stacked piezoelectric sensor with neuromorphic memory is presented. As a fundamental component for both sensors and memory, hafnium zirconium oxide (HZO) formed by using semiconductor deposition technique is introduced. Due to its exceptional piezoelectric performance, the morphotropic phase boundary of HZO is studied. The entire materials and processes are highly compatible with conventional semiconductor processes, including microwave annealing-based low-temperature crystallization. Even after 10,000 times of bending stress, the sensor and memory constructed on a flexible substrate exhibit consistent pressure detection characteristics over a wide range of 2–25 kPa. The feasibility of the approach is further demonstrated by a deep neural network simulation, which reached 90.8% braille recognition accuracy. Wearable electronics and medical devices are two examples of industrial domains that can use these flexible, exceptionally durable devices.

1. Introduction

An important step in achieving a hyper-connected society is the development of artificial tactile perception devices, which are electronic devices that imitate numerous stimuli perception components found beneath the human skin's epidermis. In particular, a system that combines a sensor with neuromorphic memory and imitates the computational process of the human brain can be used in a number of different applications, including immersive displays, robots, and medical applications.[1-6] Though there are still problems to be resolved for commercialization,[7–11] the majority of the previously described research has been on organic-based flexible sensor technologies which are not suitable for high-density and high-performance devices. Considering the density and response speed of tactile receptors in human skin, it is necessary to realize a system that can operate at high speed with high density[12] Furthermore, the majority of conventional sensor technology has been developed using micro-electro-mechanical systems (MEMS), which are not well suited for integration with silicon-based neuromorphic devices. Ferroelectric materials were developed to address this issue. Ferroelectrics are substances with pyroelectric and piezoelectric capabilities that respond to heat and pressure, respectively, and spontaneous polarization properties that persist to some extent even after the absence of an external electric field. Due to its ferroelectricity at very thin layers (4 nm) and superior compatibility with semiconductor processes compared to typical ferroelectrics like lead-zirconate-titanate (PZT) and Poly(vinylidene fluoride)-trifluoride;P(VDF-TrFE),[13-17] hafnia (HfO_2)-based materials have been explored in the memory and sensor domains. For each application, hafnia-based material composition optimization must be taken into account.

A well-known ferroelectric material with a fluorite structure is hafnium zirconium oxide (HZO). Particularly, the relationship between electrical properties and the Hf to Zr composition ratio has been thoroughly investigated in earlier reports.[18-20,47,48] Interestingly, at a particular threshold of zirconium content,

M. Jung, S. Kim, J. Hwang, S. Jeon
School of Electrical Engineering
Korea Advanced Institute of Science & Technology
Daejeon 34141, Republic of Korea
E-mail: jeonsh@kaist.ac.kr
H. J. Kim, Y. Kim
Intelligent Components and Sensors Research Section
Electronics and Telecommunications Research Institute
Daejeon 34129, Republic of Korea
J. Ahn
Division of Materials Science and Engineering
Hanyang University
Seoul 04763, Republic of Korea

The ORCID identification number(s) for the author(s) of this article can be found under https://doi.org/10.1002/aelm.202300594

DOI: 10.1002/aelm.202300594

abrupt changes in the material's piezoelectric and dielectric properties were seen. The MPB, or morphotropic phase barrier, is what causes this. In a hafnia ferroelectric system, MPB is a region where two different crystalline phases, the antiferroelectric tetragonal phase, and the ferroelectric orthorhombic phase, coexist.[21–24] The HZO films illustrate the highest capacitance value in this region with a single peak in the capacitance-voltage curve, close to zero electric field. Furthermore, the piezoelectric property is enhanced close to the MPB. Lattice instability and localized defects are related to the origin of certain material characteristics. Therefore, optimization of hafnia thin films in various thicknesses and compositions is necessary to make use of these electrical qualities close to the MPB composition for various applications. In addition, it is still difficult to establish a high-temperature annealing procedure for crystal growth to a particular crystallinity for the generation of ferroelectricity in hafnia thin films.

Compared to other traditional annealing methods, microwave annealing (MWA) can crystallize the thin film at a relatively low temperature because it exhibits volumetric heating behavior through conduction loss and dipole interaction mechanisms.[25–27] Process temperatures can be lowered when energy is applied as an electric field as opposed to directly transferring thermal energy. The advantage of MWA over lamp heating or furnace-type annealing equipment is that it has a uniform annealing characteristic from the inside of the materials to the surface, whereas those methods use thermal radiation and convection from the exterior of the materials. MWA has been employed for the crystallization and sintering of a range of materials and shapes, from bulk to powder, based on these benefits.[28,29] Additionally, electromagnetic radiation has the ability to permeate materials. As a result, many thin films can crystallize using a single annealing procedure, contributing to the speeding up and cost reduction of the production process. Due to its ability to transmit or absorb electromagnetic waves, a dielectric thin film can be used for selective thin film heating. In contrast, electromagnetic waves are reflected by a metal thin layer with a thickness of several hundred micrometers or more.

In this study, a microwave-annealed hafnia thin film is used to demonstrate an artificial touch receptor system built by semiconductor processes. There have been applications for piezoelectric sensors and nonvolatile two-terminal memory using materials based on hafnia. We used a thin film with $Hf_{0.25}Z_{0.75}O_2$ to take advantage of the high piezoelectric characteristics that show at the compound material's morphotropic phase boundary (MPB) region. In order to prevent the formation of the undesirable phase during the annealing process, a 1 nm-thick Al_2O_3 thin film was introduced into every 15 nm-thick HZO layer. A ferroelectric tunnel junction (FTJ) memory was adopted with a 6 nm-thick $Hf_{0.5}Z_{0.5}O_2$ thin film and a 3 nm-thick TaN thin film at the interface with the ferroelectric layer and bottom electrode for selector-less self-rectifying switching behavior. Since all processes were performed below 300 °C, flexible neuromorphic sensors were fabricated on inorganic-based MICA substrates. Even after a bending test with a 5 mm bending radius and more than 10 000 repeated bending cycles, the sensor's and memory's reliability characteristics remained consistent. A neurosim-based simulation that took into account the sensor's pressure sensing resolution of 2–25 kPa and tunneling electro resistance (TER) of 195.8 produced a braille recognition accuracy of 90.8%. In addition, the sensor's quick response time (8 ms) demonstrates the possibility of using a powerful artificial mechanoreceptor as a crucial component of the human–machine interface.

2. Result and Discussion

By combining sensors and neuromorphic devices, several investigations on artificial mechanoreceptors have been published.[30–32] Due to its potential for artificial neural network-based systems with low power consumption and brain processing, the module consisting of triboelectric or piezoelectric sensors and neuromorphic memory in particular has drawn enormous attention. However, due to a variety of materials used for sensors and memories, the majority of research is given through the wiring of individual devices. Flexible pressure sensors are frequently made using microstructure-based resistance change sensors, however extra power sources and slow responses need to be addressed. Additionally, it should be taken into account that the size of the sensor should look like human skin and that the pressure-detecting resolution ought to be comparable to a soft touch of 10 kPa or less. Stimulus detection and tactile recognition mechanisms and the structure of human skin are illustrated in **Figure 1a**. Here, pulse-like signals are generated from mechanoreceptors such as the Pacinian corpuscle, Meissner corpuscle, and Merkel disc in the skin in response to external stimuli and transmitted to synapses, which are the junctions between neurons.[33] More specifically, an action potential in which a signal exceeding a certain threshold point is delivered and a feedback process through the effector has occurred. To mimic this mechanism, we proposed a hafnia-based artificial tactile receptor in Figure 1b. A piezoelectric-based pressure sensor that generates a pulse-like voltage and an FTJ is connected in series to realize a neuromorphic tactile receptor system. When pressure is applied to the sensor, the generated and amplified signal is transferred to the FTJ so that the resistance level of the device is changed. Therefore, this system can be used as an artificial tactile receptor device with pressure-sensing properties. As shown in Figure 1c, a vertically stacked flexible system was fabricated on an inorganic-based MICA substrate. Hafnium zirconium oxide (HZO)-based ferroelectric material for pressure sensors and neuromorphic memory has been applied with different composition ratios and thicknesses. Polarization versus electric field (P–E) curves can represent the ferroelectric properties of HZO thin films for sensors and memory as shown in Figure 1d. Typical pinched P–E curves of HZO thin film near the MPB region for HAHAH structure and an imprinted P–E curve of 6 nm thick $Hf_{0.5}Zr_{0.5}O_2$ with a 3 nm thick lower TaN barrier for selector-less FTJ were measured.[34,35] Here, the P–E curve of FTJ was characterized in the range of 2–3 MV cm^{-1} which is the operating range of the device. According to a prior study, the elongation of the lattice's *a*-axis in fluorite structures is what causes hafnia thin films to have ferroelectric characteristics. Also, the piezoelectric effect, which is caused by the movement of oxygen ions in response to outside physical stimuli, can provide an electrical signal.[36,37] The following Equation (1), where d33 is the piezoelectric coefficient of the sensing material, capacitance (*C*), thickness (*d*), and area (*A*), respectively, can be

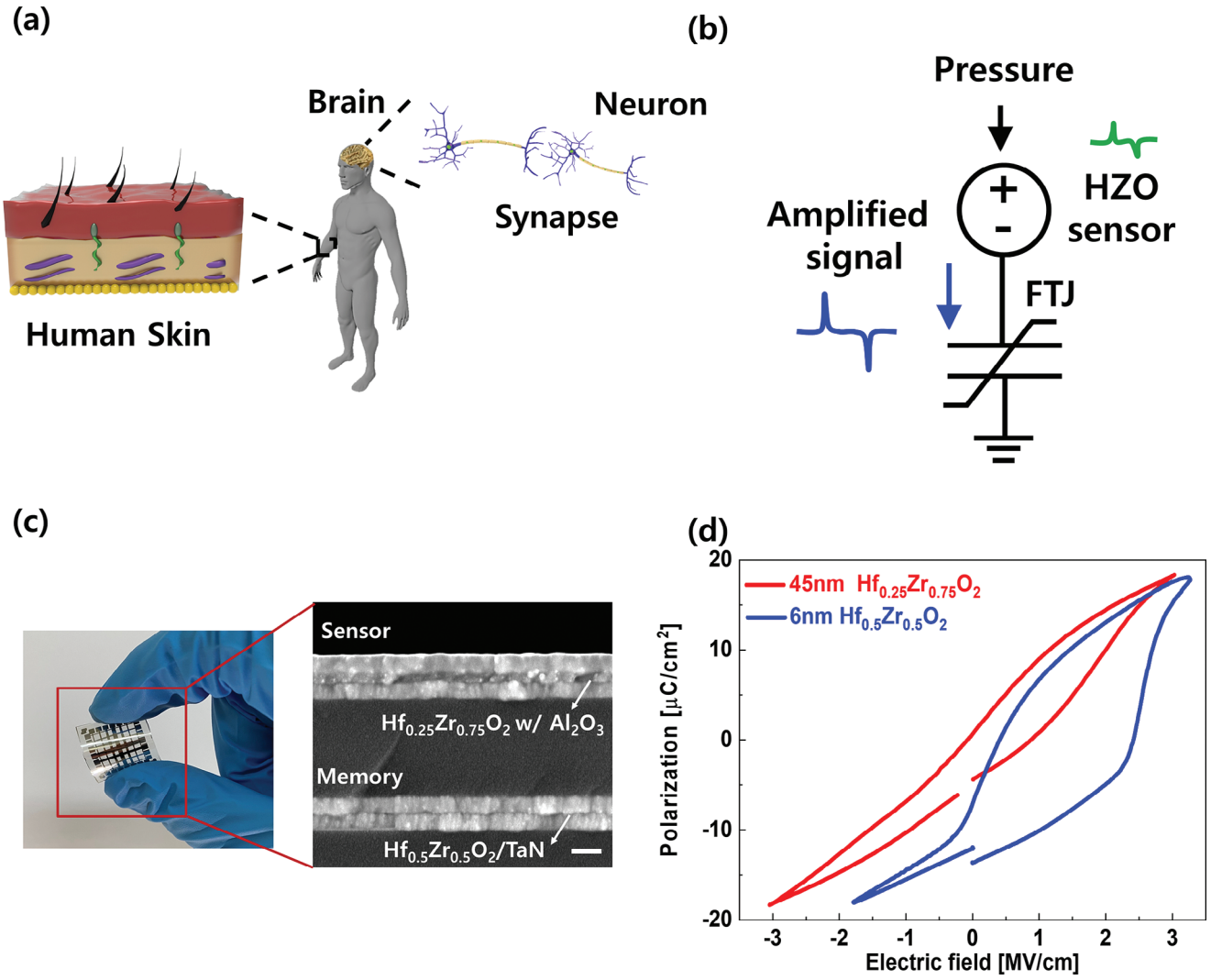

Figure 1. Structure of flexible neuromorphic pressure sensing system. Schematic of a) human stimuli sensing principle and b) HZO-based sensor and ferroelectric tunnel junction (FTJ) integrated circuit. c) Optical and scanning electron microscope images of vertically stacked systems. Scale bar: 100 nm. d) Polarization-electric field curves of the HZO layer for the pressure sensor (red) and FTJ (blue), respectively.

used to express the output voltage of the sensor with applied pressure (P).

$$V_{out} = \frac{q}{C} = \frac{d_{33}PA}{C} = \frac{d_{33}Pd}{\epsilon_0\epsilon_r} \quad (1)$$

As a pressure sensing layer, 47 nm thick $Hf_{0.25}Zr_{0.75}O_2$ including 1 nm thick Al_2O_3 inserted in every 15 nm thick HZO structure (HAHAH) was adopted to maintain the crystal structure of HZO near the MPB region which is known to have excellent piezoelectric properties. There is a restriction to expanding the thickness of HZO while preserving the particular crystalline phase, despite the fact that the pressure-sensing performance of the device is proportional to the aspect ratio. Therefore, we concentrated on the high d33 characteristics of HZO near the MPB state. The unstable lattice state is what causes the rapid amplification of piezoelectric and dielectric properties at MPB, which is a location where a ferroelectric (orthorhombic phase) and an antiferroelectric (tetragonal phase) meet.[18,24,38,39]

MWA crystallized hafnia thin films for the sensor and FTJ in the low-temperature fabrication of the device. As illustrated in **Figure 2**a, a thermocouple for temperature monitoring was designed to directly contact the sample and be used with the magnetron that produces an electromagnetic wave for 3 kW at 2.45 GHz. Additionally, hybrid annealing for homogeneous electromagnetic wave absorption was carried out using a SiC susceptor. With a 10 nm-thick $Hf_{0.5}Zr_{0.5}O_2$ thin film, an X-ray diffraction study was used to compare the crystallization of HZO thin film with MWA to traditional rapid thermal annealing (RTA). A comparable level of intensity peak was obtained for both films annealed by MWA and RTA, as illustrated in Figure 2b. We adjusted the temperature profiles of RTA and MWA for the same circumstance (temperature ramping speed: 2 °C Sec^{-1}) in order to make a more precise comparison. A typical ferroelectric hysteresis loop was achieved in a hafnia thin film that was annealed by MWA at

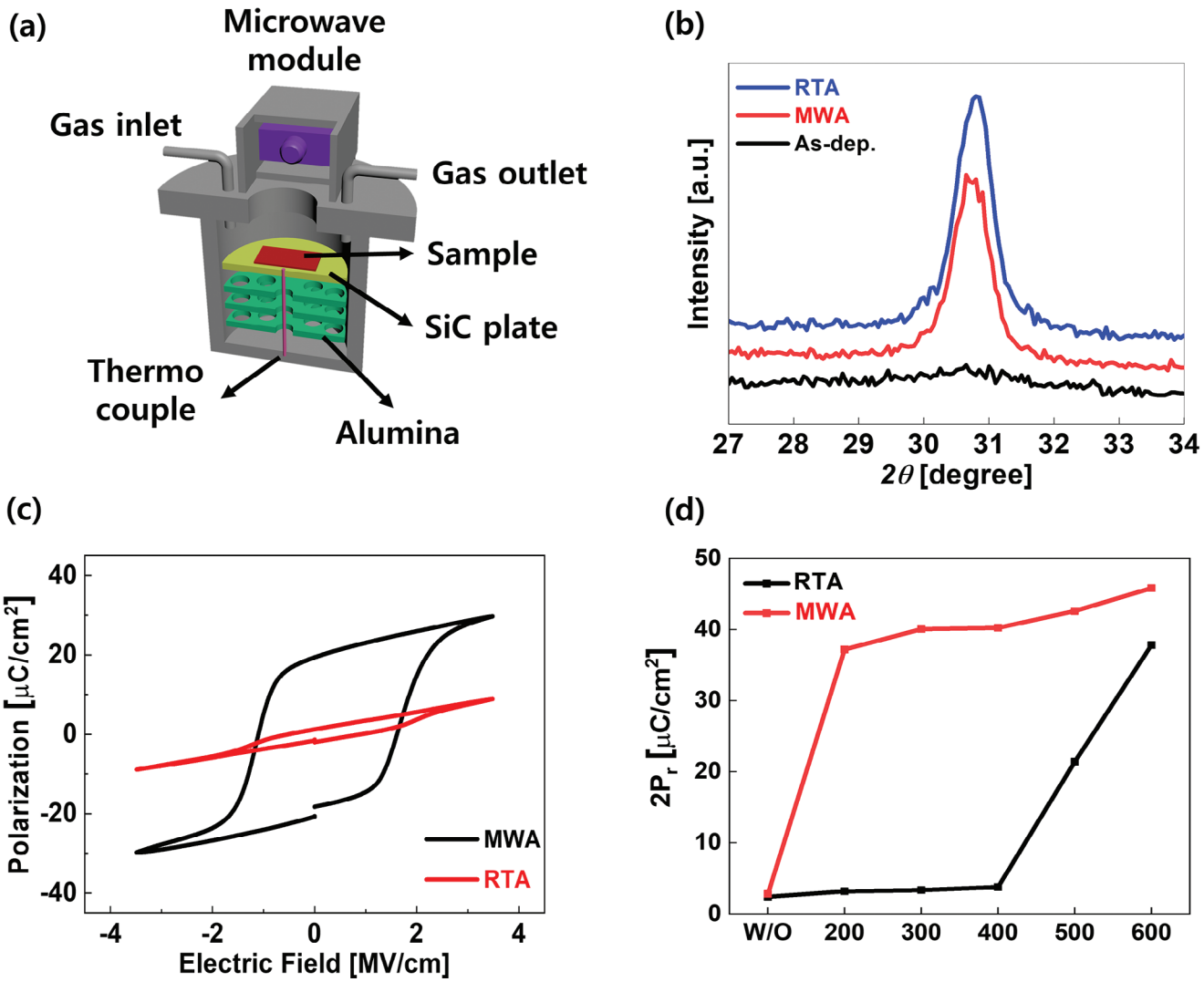

Figure 2. low-temperature crystallization of hafnia thin film for flexible applications. a) Schematic of microwave annealing (MWA) equipment. b) X-ray diffraction patterns of hafnia thin film w/ and w/o annealing process. c) Polarization versus electric field (P–E) curves of hafnia thin film annealed at 300 °C for MWA and RTA. d) Extracted remanent polarization value from the P–E curve.

300 °C, but this was not the case for films that were annealed by RTA since there was inadequate crystallization at this temperature, which led to a substantial decrease of polarization value. Figure 2d displays the extracted remanent polarization (Pr) values for various annealing temperatures. As a result, MWA promotes the crystallization of ferroelectric thin films even at low temperatures below 300 °C.

Next, we developed a pressure sensor based on a hafnia thin film. A crossbar-shaped top and bottom electrode with an area of 4 mm^2 was developed. In **Figure** 3a, the pressure sensing properties of the sensor on the Si substrate and MICA substrate were contrasted in order to assess the substrate dependence. For an accurate measurement, the pressure sensing test was carried out while the MICA substrate was glued to a glass substrate with epoxy. However, the MICA substrate's mechanical characteristics, which allow it to move vertically farther than the silicon substrate under the same pressure, lead to a greater output voltage. Figure 3b displays the quantitative output voltage with pressure. Additionally, the sensor's response time was assessed. The result was obtained by simultaneously monitoring the signal from the load cell in the pressure-applying equipment and our sensor. The response time was shown at 8 and 6 ms with the releasing and applying of pressure, respectively in Figure 3c. The piezoelectric characteristic of hafnia thin films, which we used as a pressure sensor, produces an immediate pulse-like electrical signal as a result of the movement of ions within a material lattice when the lattice is forced to move. As a result, a single-direction voltage and relaxation state are displayed when the pressure is applied in a stepwise increasing pattern without release, as shown in Figure 3d. Static pressure detection with piezoelectric sensors is also possible if these signals are put into a non-volatile memory to maintain a specific amount of resistance. We also assessed device characteristics with the application of bending force in order to confirm the applicability of low-temperature ferroelectric thin films to flexible electronics. In general, higher leakage current or electrical shorts resulting from cracks in in-

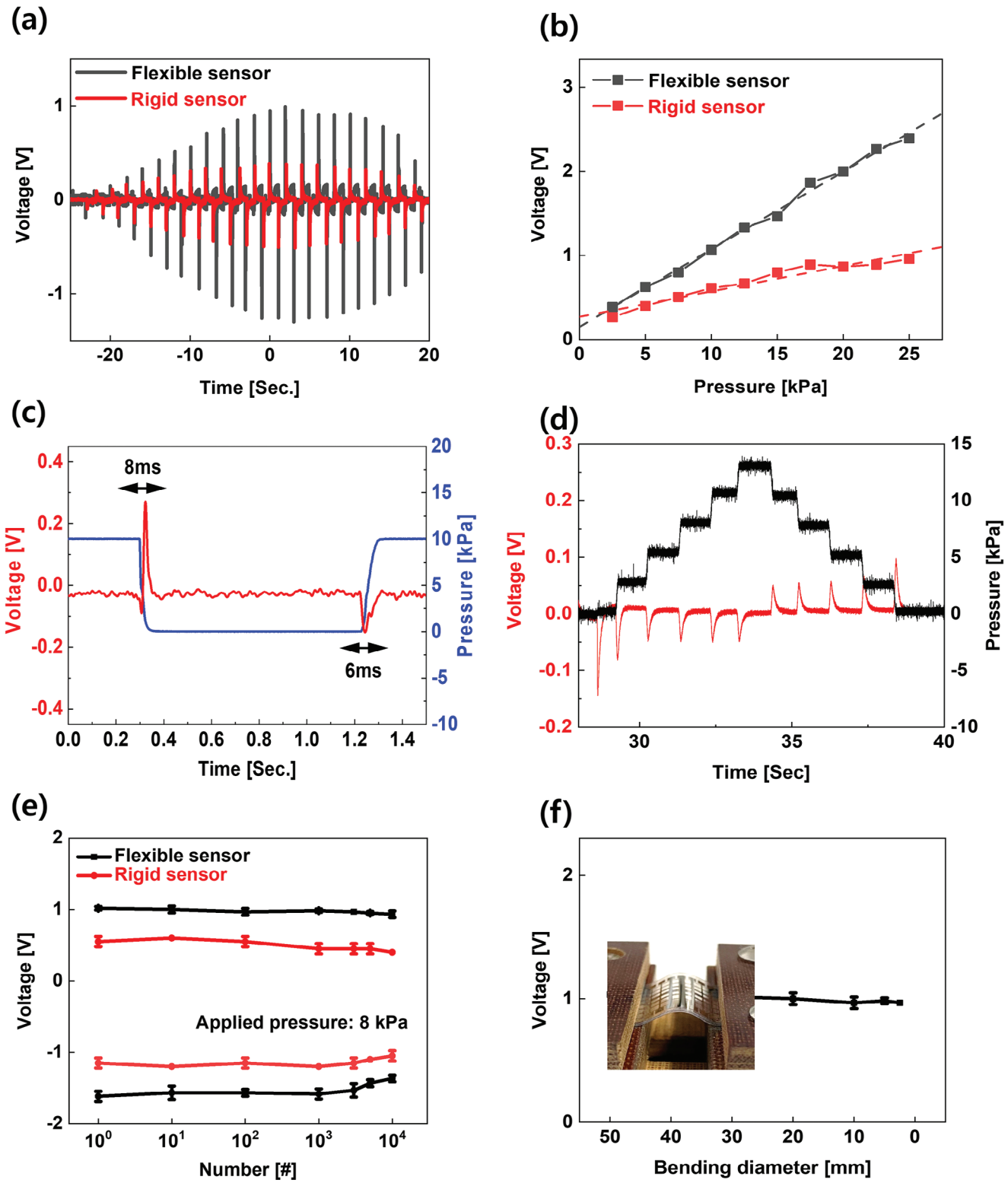

Figure 3. Pressure sensing performance of piezoelectric sensor with MPB-HZO thin film. a) The piezoelectric output voltage of the pressure sensor with gradual pressure and b) peak voltage related to quantitative pressure. c) Response time and d) nonreleased step pressure response of the sensor. Bending test of the pressure sensor with e) bending cycle and f) diameter.

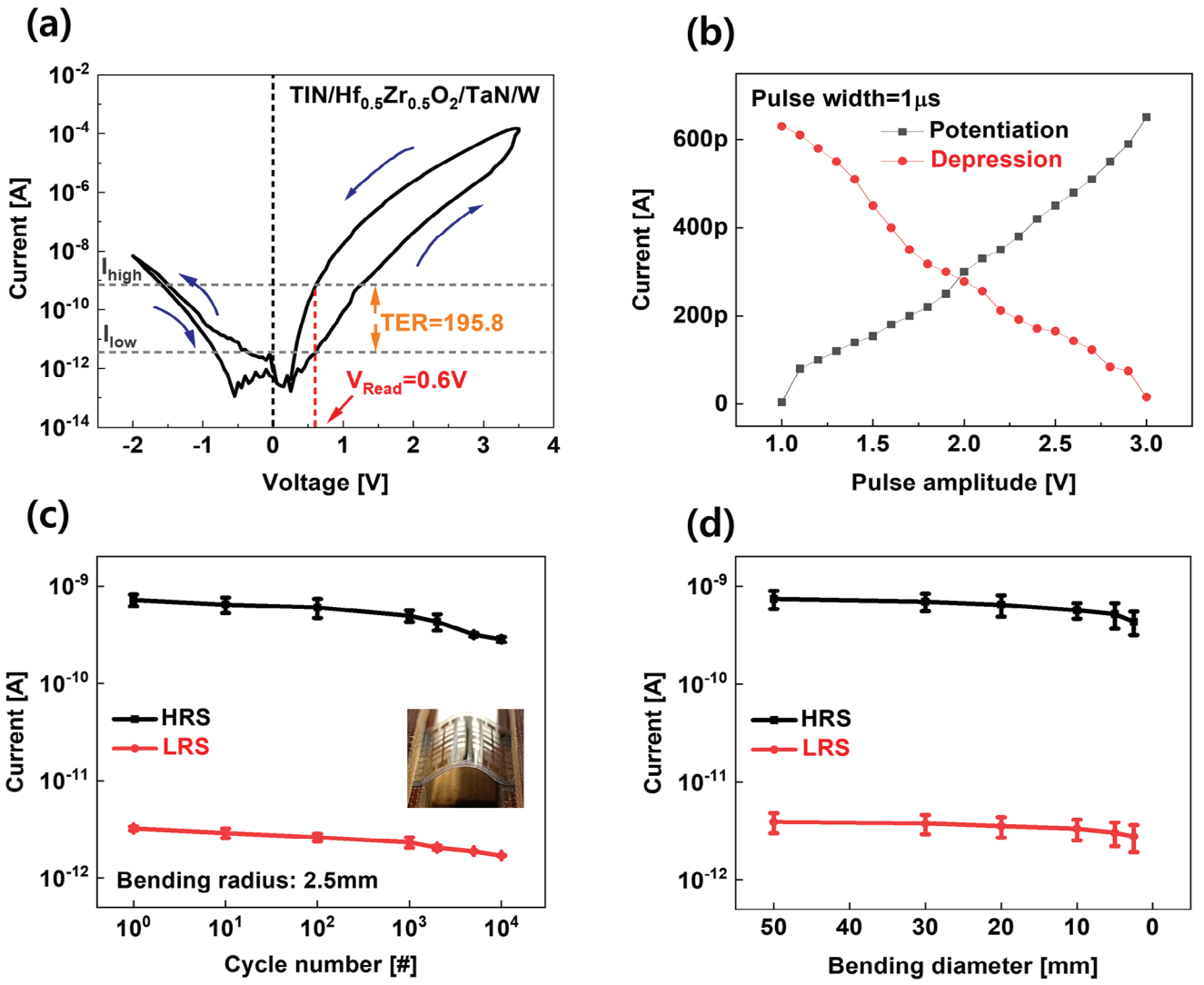

Figure 4. Electrical characteristics of ferroelectric tunnel junction (FTJ) memory. a) Current–voltage curve of FTJ and b) its potentiation and depression characteristics with amplitude modulated pulse measurement. c) and d) show the tunneling electroresistance of FTJ for bending cycles and diameter, respectively.

organic thin films cause electronic devices to degrade as a result of external physical forces. The top and bottom electrodes in this study are made of 50 nm thick TiN, while the piezoelectric sensor was made of a 47 nm thick HZO thin film. Despite the fact that all materials are inorganic, it was still able to retain some of its piezoelectric characteristics after 10 000 cycles of bending with a 5 mm bending diameter. Even at a minimum bending radius of 3 mm, which is the limit of the MICA substrate, the sensor's electrical performance did not significantly degrade (the sensor's peak voltage with bending cycles and diameter are illustrated in Figure 3e,f).

We used a hafnia-based FTJ for the neuromorphic memory component of the artificial tactile receptor. It makes use of the shift in the probability of tunneling. More specifically, tunneling electrical resistance (TER), endurance, and switching speed of FTJ can be influenced by changes in screening length related to the polarization property of the ferroelectric thin film under the electric field and the difference in work function between the metal electrode and ferroelectric layer.[40–42] Further, in polycrystalline ferroelectrics, partial domain changes can gradually alter nonvolatile electrical characteristics. In order to reduce the sneak current, we explored FTJ with a self-rectifying function in this work. It was possible to obtain it via a positive-direction horizontally-shifted hysteresis loop in the FTJ's operational electric field. According to our earlier research, the bottom TaN interlayer promotes the imprint field when the positively charged oxygen vacancies in the material create an asymmetric interfacial structure.[41] The preferential polarization state could be stabilized by such an asymmetric interface layer. At a readout voltage of 0.5 V, the TER value of 195.8 was obtained with self-rectifying behavior at the lower electrode interface of TaN. Voltage–current curves in a square-patterned device with a 100 m length were measured. The neuromorphic characteristics, such as potentiation and depression of the FTJ, were assessed by amplitude-

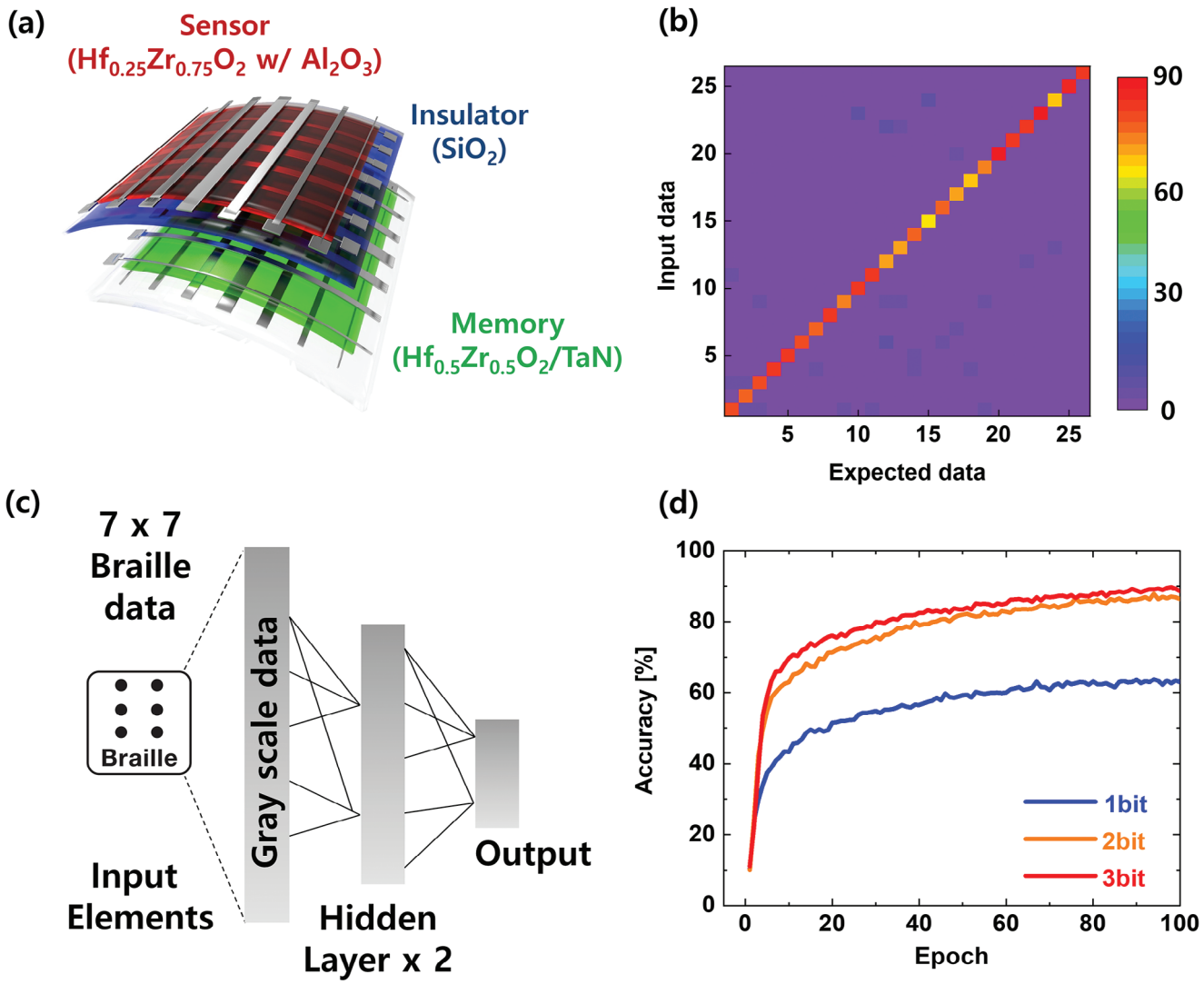

Figure 5. Neural network-based brail recognition characteristics in vertically stacked artificial tactile receptor system. a) Schematic of vertically stacked sensor and memory system. b) Brail recognition accurate mapping data from the system and c) schematic of signal processing. d) Brail recognition accurate with epoch.

modulated pulse measurement because the resistance level required to be altered through a pulse-like signal from the piezoelectric sensor. It was confirmed that linear behavior was displayed with the amplitude of the pulse voltage, as illustrated in **Figure** 4b. Since the FTJ is formed below the sensor and the ferroelectric thin film in FTJ also has piezoelectric properties, its electrical properties with external force should be considered. However, the ferroelectric thin film for FTJ (6 nm) was thinner than the layer for the sensor (≈47 nm) and $Hf_{0.5}Zr_{0.5}O_2$ for FTJ doesn't show noticeable piezoelectric performance. Thus, the piezoelectric characteristic of FTJ is ignored. Moreover, to evaluate the mechanical endurance of FTJ on a MICA substrate, a bending test similar to that for the pressure sensor was performed. As a result, we found that although the overall current flow decreased due to the increase in the resistance of the metal electrode with the number of bending cycles, the TER value was maintained at a certain level and the properties with the bending radius also showed similar behavior. Thus, we successfully demonstrated that ferroelectric thin film-based sensors and memories are applicable as flexible electronic devices.

Finally, a flexible neuromorphic pressure sensing system with a vertically stacked FTJ was fabricated and isolated in 300 nm thick SiO_2 for electrical isolation as shown in **Figure** 5a. Considering the pressure sensing resolution of the fabricated sensor and the linearity and resistance change characteristic of the FTJ, we characterized the braille recognition accuracy of our system with neurosim-based simulation.[43–45] The deep neural network (DNN) with double hidden layers was adopted for the simulation (The schematic of the simulation is shown in Figure 5c). 1000 sets of braille data prepared in 7 × 7 grayscale. As a result of applying the pressure sensing resolution of the sensor from one to three bits, braille recognition characteristics with a maximum accuracy of 90.8% were achieved in Figure 5d. Due to the limits of the data set in comparison to the handwriting recognition data

used for testing of traditional artificial neural networks, which consists of more than 10 000 data, the learning process (epoch) was repeated more than 80 times. Nonetheless, high accuracy was achieved based on the properties of the hafnia-based pressure sensor and memory. There is still room for improvement by expanding braille recognition data and increasing the pressure-sensing resolution of the sensor.

3. Conclusion

In conclusion, we suggested a flexible neuromorphic pressure sensing system based on hafnia ferroelectrics. A hafnia thin film-based piezoelectric sensor and two-terminal nonvolatile FTJ memory make up a biomimetic artificial touch receptor. The resistance level of the FTJ is altered by a pulse-like voltage from the pressure sensor in direct proportion to the applied pressure. This capacity to stack sensor and memory structures vertically allows for a gain in density and a reduction in device size. MWA carries out low-temperature ferroelectric crystallization at less than 300 °C. Even after a bending test, the pressure sensor and memory, which were built on a flexible MICA substrate, maintained a certain level of electrical characteristics and outstanding linearity throughout a broad range of 2–25 kPa. Through the use of a software-based DNN that reflects the performance of the device, a braille recognition accuracy of 90.8% was attained. Further research could increase the application of hafnia thin films through the development of thick piezoelectric films using enhanced ALD or sputtering techniques. Furthermore, raising the linearity and TER of FTJ can enhance recognition performance. Also, from the perspective of good uniformity and commercial viability, constructing wafer-level commercial microwave equipment while taking microwave dispersion into account can be a major technological achievement. We anticipate that our method for building flexible neuromorphic sensors based on hafnia will open up new possibilities for a number of industries, including haptic displays, user interfaces, healthcare, and robotics.

4. Experimental Section

Fabrication of the Flexible Neuromorphic Tactile Receptor: The ferroelectric $Hf_{0.5}Zr_{0.5}O_2$ with a thickness of 6 nm was deposited on the MICA substrate with 3 nm lower TaN barrier. After the depositioning of 300 nm of SiO_2 for electrical insulation with plasma-enhanced chemical vapor deposition (deposition temperature: 250 °C) on FTJ, the piezoelectric pressure sensing layer was deposited for the sensor. Triple-layered $Hf_{0.25}Zr_{0.75}O_2$ in which 1 nm thick Al_2O_3 was inserted in every 15 nm thick HZO thin film was adopted as MPB state HZO. HZO and Al_2O_3 thin films were deposited by plasma-enhanced atomic layer deposition at 250 °C. Precursor for each material is tetrakis(ethylmethylamino) hafnium; $Hf[N(CH_3)C_2H_5]_4$, tetrakis(ethylmethylamino) Zirconium; $Zr[N(CH_3)C_2H_5]_4$, and trimethylaluminum (TMA) $Al(CH_3)_3$ for HfO_2, ZrO_2, and Al_2O_3, respectively. All devices were fabricated in the form of crossbar array type of MFM capacitors. 50 nm thick TiN upper and lower electrodes and 3 nm thick TaN thin films were prepared through reactive sputtering with Ti and Ta targets, respectively.

Measurement Setup: The electrical characteristics of the pressure sensor were characterized by amplified and noise filtered through the low noise voltage amplifier (SR560, Stanford Research Systems), and the high-speed operation characteristics were obtained using an oscilloscope (EXR, Keysight). Pressure applying system was prepared with custom-made equipment using a commercially available load cell. A semiconductor parameter analyzer (4200A-SCS, Keithley) was used for the electrical characterization of the thin film and FTJ.

Software-Based Simulation: Deep neural network-based software simulations for the classification of braille were performed with neurosim-based open-source MATLAB code. The linearity, high resistance, low resistance (high conductance) state level of FTJ, and the sensing resolution of the pressure sensor were reflected in the simulation.

Acknowledgements

This work was supported by the National Research Foundation of Korea (No. 2021R1A2C2095322), the National Research Foundation of Korea (NRF) grant funded by the Korea government (MSIT) (Grant No. RS-2023-00260527), and the BK21 FOUR(Connected AI Education & Research Program for Industry and Society Innovation, KAIST EE, No. 4120200113769).

Conflict of Interest

The authors declare no conflict of interest.

Data Availability Statement

The data that support the findings of this study are available from the corresponding author upon reasonable request.

Keywords

artificial mechanoreceptor, E-skin, flexible electronics, HfZrO, microwave annealing

Received: September 5, 2023
Revised: November 19, 2023
Published online: January 10, 2024

[1] A. Chortos, J. Liu, Z. Bao, *Nat. Mater.* **2016**, *15*, 937.
[2] Y. Kim, A. Chortos, W. Xu, Y. Liu, J. Y. Oh, D. Son, J. Kang, A. M. Foudeh, C. Zhu, Y. Lee, S. Niu, J. Liu, R. Pfattner, Z. Bao, T.-W. Lee, *Science* **2018**, *360*, 998.
[3] Z. Lv, Y. Zhou, S.-T. Han, V. A. L. Roy, *Mater. Today* **2018**, *21*, 537.
[4] H.-L. Park, Y. Lee, N. Kim, D.-G. Seo, G.-T. Go, T.-W. Lee, *Adv. Mater.* **2020**, *32*, 1903558.
[5] C. Wan, P. Cai, M. Wang, Y. Qian, W. Huang, X. Chen, *Adv. Mater.* **2020**, *32*, 1902434.
[6] C. Wan, G. Chen, Y. Fu, M. Wang, N. Matsuhisa, S. Pan, L. Pan, H. Yang, Q. Wan, L. Zhu, X. Chen, *Adv. Mater.* **2018**, *30*, 1801291.
[7] S. H. Chae, Y. H. Lee, *Nano Converg.* **2014**, *1*, 15.
[8] J. Kim, J. Lee, D. Son, M. K. Choi, D.-H. Kim, *Nano Converg.* **2016**, *3*, 4.
[9] S. Jeon, S.-C. Lim, T. Q. Trung, M. Jung, N.-E. Lee, *Proceed. IEEE* **2019**, *107*, 2065.
[10] C. Parameswaran, D. Gupta, *Nano Converg.* **2019**, *6*, 28.
[11] M. Jung, J. Lee, S. K. Vishwanath, O.-S. Kwon, C. W. Ahn, K. Shin, S. Jeon, *Flex. Print. Electron.* **2020**, *5*, 025003.
[12] W. Taube Navaraj, C. García Nunez, D. Shakthivel, V. Vinciguerra, F. Labeau, D. H. Gregory, R. Dahiya, *Front. Neurosci.* **2017**, *11*, 501.
[13] K.-I. Park, J. H. Son, G.-T. Hwang, C. K. Jeong, J. Ryu, M. Koo, I. Choi, S. H. Lee, M. Byun, Z. L. Wang, K. J. Lee, *Adv. Mater.* **2014**, *26*, 2514.
[14] D. Dhakras, Y. Gawli, S. Chhatre, P. Wadgaonkar, S. Ogale, *Phys. Chem. Chem. Phys.* **2014**, *16*, 22874.

[15] H. He, Y. Fu, W. Zang, Q. Wang, L. Xing, Y. Zhang, X. Xue, *Nano Energy* **2017**, *31*, 37.
[16] J. Park, M. Kim, Y. Lee, H. S. Lee, H. Ko, *Sci. Adv.* **2015**, *1*, e1500661.
[17] H. S. Wang, S. K. Hong, J. H. Han, Y. H. Jung, H. K. Jeong, T. H. Im, C. K. Jeong, B.-Y. Lee, G. Kim, C. D. Yoo, K. J. Lee, *Sci. Adv.* **2021**, *7*, eabe5683.
[18] M. Jung, V. Gaddam, S. Jeon, *Nano Converg.* **2022**, *9*, 44.
[19] A. Kashir, H. Hwang, *Phys. Status Solidi* **2021**, *218*, 2000819.
[20] M. H. Park, D. H. Lee, K. Yang, J.-Y. Park, G. T. Yu, H. W. Park, M. Materano, T. Mittmann, P. D. Lomenzo, T. Mikolajick, U. Schroeder, C. S. Hwang, *J. Mater. Chem. C* **2020**, *8*, 10526.
[21] D. Das, B. Buyantogtokh, V. Gaddam, S. Jeon, *IEEE Trans. Electron Devices* **2021**, *69*, 103.
[22] V. Gaddam, G. Kim, T. Kim, M. Jung, C. Kim, S. Jeon, *ACS Appl. Mater. Interfaces* **2022**, *14*, 43463.
[23] S. Kim, S. H. Lee, M. J. Kim, W. S. Hwang, H. S. Jin, B. J. Cho, *IEEE Electron Device Lett.* **2021**, *42*, 517.
[24] M. H. Park, Y. H. Lee, H. J. Kim, Y. J. Kim, T. Moon, K. D. Kim, S. D. Hyun, C. S. Hwang, *ACS Appl. Mater. Interfaces* **2018**, *10*, 42666.
[25] E.-K. Hong, W.-J. Cho, *Microelectron. Reliab.* **2018**, *80*, 306.
[26] T. L. Alford, M. J. Gadre, R. N. P. Vemuri, N. D. Theodore, *Thin Solid Films* **2012**, *520*, 4314.
[27] C. Fu, Y. Wang, P. Xu, L. Yue, F. Sun, D. W. Zhang, S.-L. Zhang, J. Luo, C. Zhao, D. Wu, *AIP Adv.* **2017**, *7*, 035214.
[28] M. Bhattacharya, T. Basak, *Energy* **2016**, *97*, 306.
[29] R. R. Mishra, A. K. Sharma, *Composites, Part A* **2016**, *81*, 78.
[30] M. Wang, Y. Luo, T. Wang, C. Wan, L. Pan, S. Pan, K. He, A. Neo, X. Chen, *Adv. Mater.* **2021**, *33*, 2003014.
[31] X. Zhang, Y. Zhuo, Q. Luo, Z. Wu, R. Midya, Z. Wang, W. Song, R. Wang, N. K. Upadhyay, Y. Fang, F. Kiani, M. Rao, Y. Yang, Q. Xia, Q. Liu, M. Liu, J. J. Yang, *Nat. Commun.* **2020**, *11*, 51.
[32] X.-F. Zhao, C.-Z. Hang, H.-L. Lu, K. Xu, H. Zhang, F. Yang, R.-G. Ma, J.-C. Wang, D. W. Zhang, *Nano Energy* **2020**, *68*, 104346.
[33] Y. H. Jung, J.-H. Kim, J. A. Rogers, *Adv. Funct. Mater.* **2021**, *31*, 2008805.
[34] A. Kashir, H. Hwang, *Nanotechnology* **2021**, *32*, 445706.
[35] M. H. Park, H. J. Kim, Y. J. Kim, Y. H. Lee, T. Moon, K. D. Kim, S. D. Hyun, C. S. Hwang, *Appl. Phys. Lett.* **2015**, *107*, 192907.
[36] T. S. Böscke, J. Müller, D. Bräuhaus, U. Schröder, U. Böttger, *Appl. Phys. Lett.* **2011**, *99*, 102903.
[37] M. H. Park, T. Schenk, C. M. Fancher, E. D. Grimley, C. Zhou, C. Richter, J. M. Lebeau, J. L. Jones, T. Mikolajick, U. Schroeder, *J. Mater. Chem. C* **2017**, *5*, 4677.
[38] M. Iwata, Y. Ishibashi, *Jpn. J. Appl. Phys.* **2000**, *39*, 5156.
[39] J. Y. Park, D. H. Lee, K. Yang, S. H. Kim, G. T. Yu, G. H. Park, E. B. Lee, K. H. Kim, M. H. Park, *ACS Appl. Electron. Mater.* **2021**, *4*, 1369.
[40] Y. Goh, J. Hwang, M. Kim, M. Jung, S. Lim, S.-O. Jung, S. Jeon, In *2021 IEEE Int. Electron Devices Meeting (IEDM)*, **2021**, IEEE, New York: pp 17.2.1–17.2.4.
[41] Y. Goh, J. Hwang, M. Kim, Y. Lee, M. Jung, S. Jeon, *ACS Appl. Mater. Interfaces* **2021**, *13*, 59422.
[42] Y. Goh, J. Hwang, Y. Lee, M. Kim, S. Jeon, *Appl. Phys. Lett.* **2020**, *117*, 242901.
[43] P.-Y. Chen, X. Peng, S. Yu, in *IEEE Transactions Computer-Aided Design Integrated Circuits Systems*, IEEE, New York **2018**, 3067.
[44] P.-Y. Chen, X. Peng, S. Yu, In *2017 IEEE Int. Electron Devices Meeting (IEDM)*, IEEE, New York **2017**, pp 6.1–6.4.
[45] S. Choi, S. H. Tan, Z. Li, Y. Kim, C. Choi, P.-Y. Chen, H. Yeon, S. Yu, J. Kim, *Nat. Mater.* **2018**, *17*, 335.
[46] J. Lee, K. Yang, J. Y. Kwon, J. E. Kim, D. I. Han, D. H. Lee, J. H. Yoon, M. H. Park, *Nano Convergence* **2023**, *10*, https://doi.org/10.1186/s40580-023-00403-4.
[47] M. Hellenbrand, J. MacManus-Driscoll, *Nano Convergence* **2023**, *10*, https://doi.org/10.1186/s40580-023-00392-4.
[48] Z. Zhang, W. Kim, M. J. Ko, Y. Li, *Nano Convergence* **2023**, *10*, https://doi.org/10.1186/s40580-023-00373-7.